

# Lattice QCD thermodynamic results with improved staggered fermions

Christian Schmidt<sup>1</sup> for RBC-Bielefeld and HotQCD Collaborations

Fakultät für Physik, Universität Bielefeld, D-33615 Bielefeld, Germany

Received: date / Revised version: date

**Abstract.** We present results on the QCD equation of state, obtained with two different improved dynamical staggered fermion actions and almost physical quark masses. Lattice cut-off effects are discussed in detail as results for three different lattice spacings are available now, i.e. results have been obtained on lattices with temporal extent of  $N_\tau = 4, 6$  and  $8$ . Furthermore we discuss the Taylor expansion approach to non-zero baryon chemical potential and present the isentropic equation of state on lines of constant entropy per baryon number.

**PACS.** 11.15.Ha Lattice gauge theory – 11.10.Wx Finite-temperature field theory – 12.38.Gc Lattice QCD calculations – 12.38.Mh Quark-gluon plasma

## 1 Introduction

A detailed and comprehensive understanding of the thermodynamics of quarks and gluons, e.g. of the equation of state is most desirable and of particular importance for the phenomenology of relativistic heavy ion collisions. Lattice regularized QCD simulations at non-zero temperatures have been shown to be a very successful tool in analyzing the non-perturbative features of the quark-gluon plasma. Driven by both, the exponential growth of the computational power of recent super-computer as well as by drastic algorithmic improvements one is now able to simulate dynamical quarks and gluons on fine lattices with almost physical masses.

In this article we present results on bulk thermodynamic quantities and the equation of state on lattices with temporal extent of  $N_\tau = 4, 6$  [1] and preliminary results on  $N_\tau = 8$ , obtained by the HotQCD collaboration [2,3]. The article is organized as follows, in Sec. 2 we discuss details of our lattice actions and corresponding finite cut-off corrections, in Sec. 3 we present our choice of lattice parameter, in Sec. 4 we present preliminary results on the equation of state and in Sec. 5 we introduce the Taylor expansion method and calculate leading and next to leading order corrections of bulk thermodynamic quantities to a non-zero baryon chemical potential. Finally, we present our preliminary results on the isentropic equation of state in Sec. 6 and conclude in Sec. 7.

## 2 Choice of action and cut-off effects

In order to control lattice cut-off effects it is of particular importance for finite temperature calculations to improve

the lattice action beyond the naive discretization scheme. As most bulk thermodynamic observables, like the energy density and pressure, are dimension four operators, the numerical signal for these observables drops like the lattice spacing to the fourth power. One is forced to perform lattice calculations on rather coarse lattices, where cut-off effects are still sizable. Using an improvement scheme as introduced by Symanzik [4] for the gauge part of the action and similarly for the fermionic part in the case of staggered fermions [5,6] or Wilson type fermions [7,8,9], cut-off effects can be drastically reduced. By adding irrelevant operators to the action which will vanish in the continuum limit, cut-off effect to arbitrary order in  $\mathcal{O}(a^n)$  can be eliminated already for finite lattice spacing  $a$ . The above mentioned improvement schemes for staggered fermions are tree-level improvements  $\mathcal{O}(g^0)$  but can in principle be generalized to eliminate cut-off effect also in leading order of the gauge coupling  $\mathcal{O}(g^2)$ .

The basis for the two actions we will consider here is given by two versions of  $\mathcal{O}(a^2 g^0)$  improved staggered fermions which contain quark and anti-quark fields separated by up to three links. By adding a straight 3-link term to the standard 1-link term, and choosing the coefficient such that the leading order cut-off effects cancel, one arrives at the Naik action [5]. Using bended 3-link terms instead (knight moves), one derives the p4 action [6]. The latter action has a dispersion relation which is  $\mathcal{O}(p^4)$  improved.

In addition to the tree-level improvements one introduces a smeared 1-link term which reduces the flavor symmetry breaking of the staggered fermions. In case of the p4-action, the 1-link term is smeared by the sum of all corresponding 3-link staples. In case of the Naik action, staples up to length of 7 links are used as well as an addi-

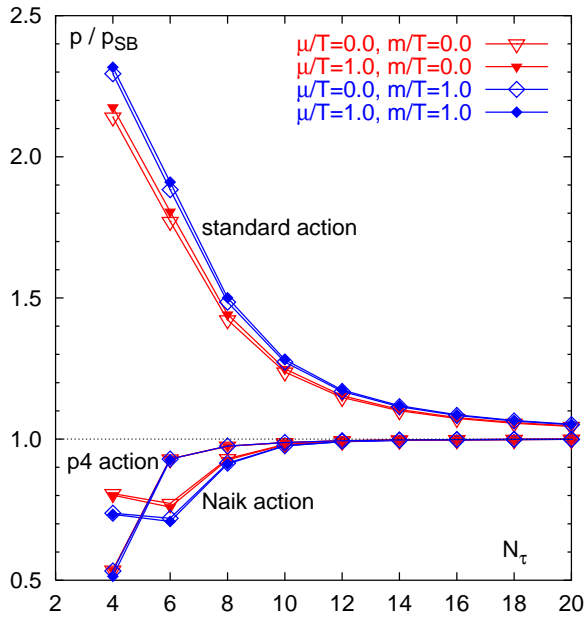


**Fig. 1.** Pressure for three different types of free lattice fermions as function of  $N_\tau$ . Results are given in units of the continuum ideal Fermi gas value and are calculated for two different masses and two different values of chemical potentials.

tional tadpole improvement (1-loop level). The gauge part of both actions is Symanzik improved. Using all this improvements together these actions are called p4fat3 and asqtad, respectively.

In the free gas limit ( $T \rightarrow \infty$ ), where the smearing becomes irrelevant, the cut-off effects of the p4 and Naik actions for bulk thermodynamic quantities have been analyzed in detail [10]. Within a large  $N_\tau$  expansion, where  $N_\tau$  is the number of lattice sites in temporal direction one can quantify how the pressure approaches its continuum (Stefan-Boltzmann) value  $p_{SB}$ . In comparison we find for the standard (non-improved), p4 and the Naik actions

$$\begin{aligned}
 \frac{p}{p_{SB}} &= 1 + \frac{248}{147} \left(\frac{\pi}{N_\tau}\right)^2 + \frac{635}{147} \left(\frac{\pi}{N_\tau}\right)^4 + \dots & (\text{std}) \\
 \frac{p}{p_{SB}} &= 1 + 0 - \frac{1143}{980} \left(\frac{\pi}{N_\tau}\right)^4 + \frac{73}{2079} \left(\frac{\pi}{N_\tau}\right)^6 + \dots & (\text{p4}) \\
 \frac{p}{p_{SB}} &= 1 + 0 - \frac{1143}{980} \left(\frac{\pi}{N_\tau}\right)^4 - \frac{365}{77} \left(\frac{\pi}{N_\tau}\right)^6 + \dots & (\text{Naik})
 \end{aligned} \tag{1}$$

As one can see, the leading order corrections of the improved p4 and Naik actions are identical. However, the sub-leading coefficient which is of order  $(\pi/N_\tau)^6$  is much smaller for p4 than for the Naik action. In Fig 1 we show the exact evaluation of the pressure as function of  $N_\tau$ , for two different masses and two different chemical potentials. It is evident, that the dependence of cut-off effects on quark mass and chemical potential  $\mu$  is very small and similar in all three discretization schemes. In fact, one can show that the dependence of finite cut-off corrections on  $\mu$  is given by Bernoulli polynomials and is independent of the discretization schemes [10].

### 3 Lattice parameter and scale setting

We perform calculations on lattices of extent  $16^3 \times 4$ ,  $24^3 \times 6$ , using the p4fat3 action [1] and  $32^3 \times 8$  with both p4fat3 and asqtad actions. The latter calculations are still preliminary and are currently performed by the HotQCD collaboration [2]. For the generation of gauge configurations we use the exact RHMC algorithm [11]. For each finite temperature calculation we perform a corresponding zero temperature calculation on a lattice of at least the size  $N_\sigma^4$ , where  $N_\sigma$  is the spatial extent of the finite temperature calculation.

The simulations are done on a line of constant physics (LCP), i.e. the quark masses are kept constant in physical units. In practice, this has been obtained by tuning the bare quark masses such that the meson masses of e.g. pion, kaon and pseudo-scalar strange meson  $\bar{s}s$  stay constant in the QCD vacuum as we change the value of the coupling. The strange quark mass was always fixed to its physical value, by fixing kaon and  $\bar{s}s$  to their corresponding physical values [1]. We find that the LCP can, to a good approximation, be parameterized by a constant ratio of the bare quark masses. Most calculation are done on a LCP which corresponds to a pion mass of about 220 MeV. We do, however, also show preliminary results with a physical pion mass, i.e.  $m_\pi \approx 150$  MeV.

To set the temperature scale in physical units, we determine two distance scales,  $r_0$  and  $r_1$ , from the zero temperature static quark potential

$$\left( r^2 \frac{dV_{\bar{q}q}(r)}{dr} \right)_{r=r_0} = 1.65, \quad \left( r^2 \frac{dV_{\bar{q}q}(r)}{dr} \right)_{r=r_1} = 1.0 \tag{2}$$

The ratio of both scales is only slightly quark mass dependent. It has been determined in both discretization schemes consistently,  $r_0/r_1 = 1.4636(60)$  (p4fat3 [1]) and  $1.474(7)(18)$  (asqtad [12]). The distance scales  $r_0$  and  $r_1$  have been related to properties of the charmonium spectrum which allows to determine them in physical units. We use here  $r_0 = 0.469(7)$  fm as determined in Ref. [13]. More details on the scale setting procedure, as well as the parameterization of the LCP are given in Ref. [1].

### 4 The equation of state

Along the line of constant physics, at sufficiently large volume and at zero chemical potential, the temperature is the only intensive parameter that controls the thermodynamics. Consequently there exists only one independent bulk thermodynamic observable that needs to be calculated. All other quantities are then obtained by using standard thermodynamic relations. On the lattice, it is convenient to first calculate the trace anomaly in units of the fourth power of the temperature,  $\Theta^{\mu\mu}/T^4$ . It is easily obtained as a derivative of the pressure  $p/T^4$ , with respect to the temperature,

$$\frac{\Theta^{\mu\mu}}{T^4} \equiv \frac{\epsilon - 3p}{T^4} = T \frac{\partial}{\partial T} (p/T^4). \tag{3}$$

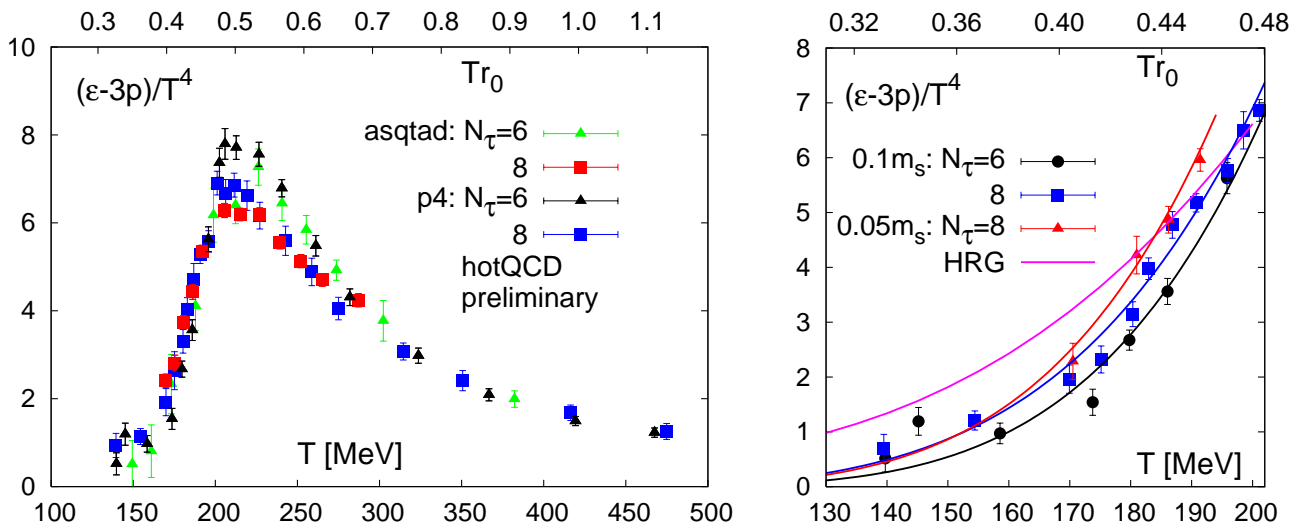


**Fig. 2.** The trace anomaly,  $(\epsilon - 3p)/T^4$  on  $N_\tau = 6$  and  $8$  lattices. On the left panel results are obtained with the p4fat3 and asqtad actions, where  $N_\tau = 6$  results are from [1] and [14] respectively,  $N_\tau = 8$  results are preliminary hotQCD results [2]. The right panel shows the low temperature part of the trace anomaly in detail, here we plot only results obtained by the p4fat3 action. Also shown on the right panel are quadratic fits to the data, as well as the trace anomaly obtained in the framework of the Resonance gas model. Light quark masses have been constrained to be one tenth of the strange quark mass ( $0.1m_s$ ), on the right panel we show, however, also preliminary results from simulations with physical quark masses ( $0.05m_s$ ).

As the pressure is directly given by the partition function,  $p/T = V^{-1} \ln Z$ , the calculation of the trace anomaly requires only the evaluation of rather simple expectation values. According to Eq. 3 one then obtains the pressure by

$$\frac{p(T)}{T^4} - \frac{p(T_0)}{T_0^4} = \int_{T_0}^T dT' \frac{1}{T'^5} \Theta^{\mu\mu}(T'). \quad (4)$$

Here  $T_0$  is an arbitrary temperature value which usually is chosen in the low temperature regime where the pressure and other thermodynamic quantities are suppressed exponentially by Boltzmann factors corresponding to the lightest hadronic states; e.g. the pions. The energy density is then obtained by combining results for  $p/T^4$  and  $(\epsilon - 3p)/T^4$ , respectively.

In Fig. 2 (left) we show results for  $\Theta^{\mu\mu}/T^4$  obtained with the asqtad and p4fat3 actions, respectively. The new  $N_\tau = 8$  results [2] are compared to  $N_\tau = 6$  results taken from [1, 14]. We note that the asqtad and p4fat3 formulations give results which are in good agreement with each other. In fact, in quite a large temperature regime the agreement for given lattice extent  $N_\tau$  seems to be better than one could expect in view of the overall cut-off dependence that is visible when comparing results for  $N_\tau = 6$  and  $N_\tau = 8$  more closely. They lead to a reduction of the peak height in  $\Theta^{\mu\mu}/T^4$ , which is located at  $T \simeq 200$  MeV and to a shift of the rapidly rising part of  $\Theta^{\mu\mu}/T^4$  in the transition region to smaller values of the temperature.

In Fig. 2 (right) we show quadratic fits to the data obtained by the p4fat3 action, to highlight the cut-off effects. It is evident, that the  $N_\tau = 8$  data is shifted relative to the  $N_\tau = 6$  data by about 8 MeV at low temperatures,

$T \simeq 160$  MeV. This shift decreases to about 5 MeV at temperatures  $T \simeq 190$  MeV.

Light quark masses have been constrained to be one tenth of the strange quark mass ( $0.1m_s$ ), on the right panel we show, however, also preliminary results from simulations with physical quark masses ( $0.05m_s$ ). This again leads to a further shift in  $\Theta^{\mu\mu}$  of approximately 5 MeV at  $T \simeq 190$  MeV towards lower temperatures.

We also compare the results for  $(\epsilon - 3p)/T^4$  to results obtained from the hadron resonance gas model. Details on the resonance gas curve in Fig. 2 (right) will be given in [2]. The slope of  $(\epsilon - 3p)/T^4$  obtained by the resonance gas model seems to be much smaller than the slope obtained by the quadratic fits to the data. Whether this points at deviations of the equation of state at lower temperatures from resonance gas behavior or is due to larger cut-off effects in the low temperature regime requires further studies. We note that the lattice spacing becomes larger at lower temperatures and violations of flavor symmetry, which are inherent to the staggered fermion formulations at finite lattice spacing, thus may become more important.

The cut-off dependence observed in  $\Theta^{\mu\mu}/T^4$  carries over to the calculation of pressure and energy density; the former is obtained by integrating over  $\Theta^{\mu\mu}/T^5$  and the energy density is then obtained by combining results for  $p/T^4$  and  $(\epsilon - 3p)/T^4$ . This is apparent in Fig. 3 where we show the ratio  $p/\epsilon$  obtained with the p4fat3 action on  $N_\tau = 6$  [1] and  $N_\tau = 8$  [2] lattices. Cut-off effects are still visible in the vicinity of the 'softest point' of the EoS, which is related to the peak position of  $(\epsilon - 3p)/T^4$ . We find that in the entire range of energy densities relevant for the expansion of dense matter created at RHIC,

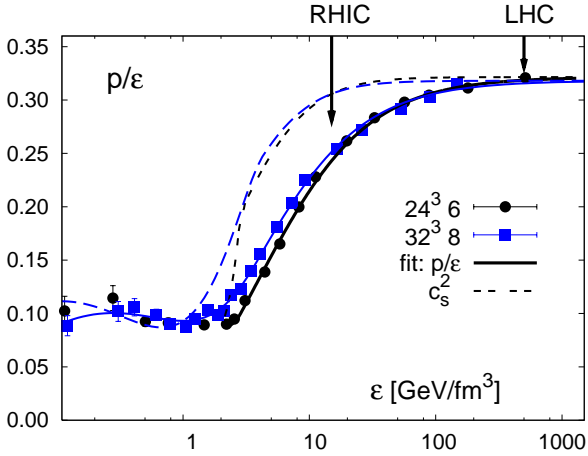


**Fig. 3.** The ratio of pressure and energy density as well as the velocity of sound obtained in calculations with the p4fat3 action on  $N_\tau = 6$  [1] and  $N_\tau = 8$  [2] lattices.

$\epsilon \lesssim 10 \text{ GeV/fm}^3$ , the ratio  $p/\epsilon$  deviates significantly from the conformal, ideal gas value  $p/\epsilon = 1/3$ .

This also is reflected in the behavior of the velocity of sound,  $c_s^2 = dp/d\epsilon$ , which is shown in Fig. 3 by dashed lines. It starts deviating significantly from the ideal gas value below  $\epsilon \simeq 10 \text{ GeV/fm}^3$  and reaches a value of about 0.1 in the transition region at energy densities  $\epsilon \simeq 1 \text{ GeV/fm}^3$ . Below the transition it slightly rises again, but note, that for very small temperatures  $c_s^2$ , as well as  $p/\epsilon$  are sensitive the integration constant  $p_0(T_0)$  (see Eq. 3). At present we have set  $p_0(T_0) = 0$ , for  $T_0 = 100 \text{ MeV}$ .

## 5 Non-zero chemical potential

At non-zero chemical potential, lattice QCD is harmed by the “sign-problem”, which makes direct lattice calculations with standard Monte Carlo techniques at non-zero density practically impossible. However, for small values of the chemical potential, some methods have been successfully used to extract information on the dependence of thermodynamic quantities on the chemical potential. For an overview see, e.g. [15].

We closely follow here the approach and notation used in Ref. [16]. We start with a Taylor expansion for the pressure in terms of the quark chemical potentials

$$\frac{p}{T^4} = \sum_{i,j,k} c_{i,j,k}^{u,d,s}(T) \left(\frac{\mu_u}{T}\right)^i \left(\frac{\mu_d}{T}\right)^j \left(\frac{\mu_s}{T}\right)^k. \quad (5)$$

The expansion coefficients  $c_{i,j,k}^{u,d,s}(T)$  are computed on the lattice at zero chemical potential, using stochastic estimators. Some details are given in [17].

In Fig. 4 we show results on the diagonal expansion coefficients with respect to the up-quark chemical potential up to the six order ( $c_{n,0,0}^{u,d,s}$  with  $n = 2, 4, 6$ ), obtained with the p4fat3 action. Here the full symbols are from  $N_\tau = 4$  lattices, while the open symbols denote results

from  $N_\tau = 6$  lattices. We find that cut-off effects are small and of similar magnitude as those found for the trace anomaly  $\Theta^{\mu\mu}$ . This was already anticipated by the analysis of the cut-off corrections in the free gas limit. Similar results for the asqtad action have been obtained in [18].

We also compare our preliminary results for 2+1-flavor QCD and a pion mass of  $m_\pi \approx 220 \text{ MeV}$ , with previously obtained result of 2-flavor QCD and  $m_\pi \approx 770 \text{ MeV}$  [16] (also p4fat3 and  $N_\tau = 4$ ). It is apparent from Fig. 4 that the critical temperature for these two particular sets of lattice parameter differ substantially and in fact decreases from about 225 MeV for the heavier mass calculations to about 200 MeV for the lighter mass calculations. Note, that those  $T_c$  values are the  $N_\tau = 4$  values, which of course are still influenced by the finite lattice spacing. Furthermore, we find from Fig. 4 that the quark number fluctuations of second, fourth and sixth order, which are related to those expansion coefficients, increase with decreasing quark mass.

Alternatively to the quark chemical potentials one can introduce chemical potentials for the conserved quantities baryon number  $B$ , electric charge  $Q$  and strangeness  $S$  ( $\mu_{B,Q,S}$ ), which are related to  $\mu_{u,d,s}$  via

$$\mu_u = \frac{1}{3}\mu_B + \frac{2}{3}\mu_Q, \quad (6)$$

$$\mu_d = \frac{1}{3}\mu_B - \frac{1}{3}\mu_Q, \quad (7)$$

$$\mu_s = \frac{1}{3}\mu_B - \frac{1}{3}\mu_Q - \mu_S. \quad (8)$$

By means of these relations the coefficients  $c_{i,j,k}^{B,Q,S}$  of the pressure expansion in terms of  $\mu_{B,Q,S}$  are easily obtained, in analogy to Eq. 5

$$\frac{p}{T^4} = \sum_{i,j,k} c_{i,j,k}^{B,Q,S}(T) \left(\frac{\mu_B}{T}\right)^i \left(\frac{\mu_Q}{T}\right)^j \left(\frac{\mu_S}{T}\right)^k. \quad (9)$$

For the rest of this article we will restrict ourselves to the case of  $\mu_Q \equiv \mu_S \equiv 0$ , thus we will suppress in the following the indices that are related to those chemical potentials. From the pressure we immediately obtain the baryon number density  $n_B$ , which is given by the derivative of  $p/T^4$  with respect to the baryon chemical potential  $\mu_B$  and can be expressed in term of the expansion coefficients  $c_n^B$ , we have

$$\frac{n_B}{T^3} = \sum_{n=2}^{\infty} n c_n^B(T) \left(\frac{\mu_B}{T}\right)^{n-1}. \quad (10)$$

Using standard thermodynamic relations we can also calculate the expansion coefficients of the trace anomaly  $\Theta^{\mu\mu}$  or equivalently the difference between energy density and three times the pressure,

$$\frac{\epsilon - 3p}{T^4} = \sum_{n=0}^{\infty} \bar{c}_n^B(T) \left(\frac{\mu_B}{T}\right)^n, \quad (11)$$

where the expansion coefficients  $\bar{c}_n^B$  are given by

$$\bar{c}_n^B(T) = T \frac{dc_n^B(T)}{dT}. \quad (12)$$

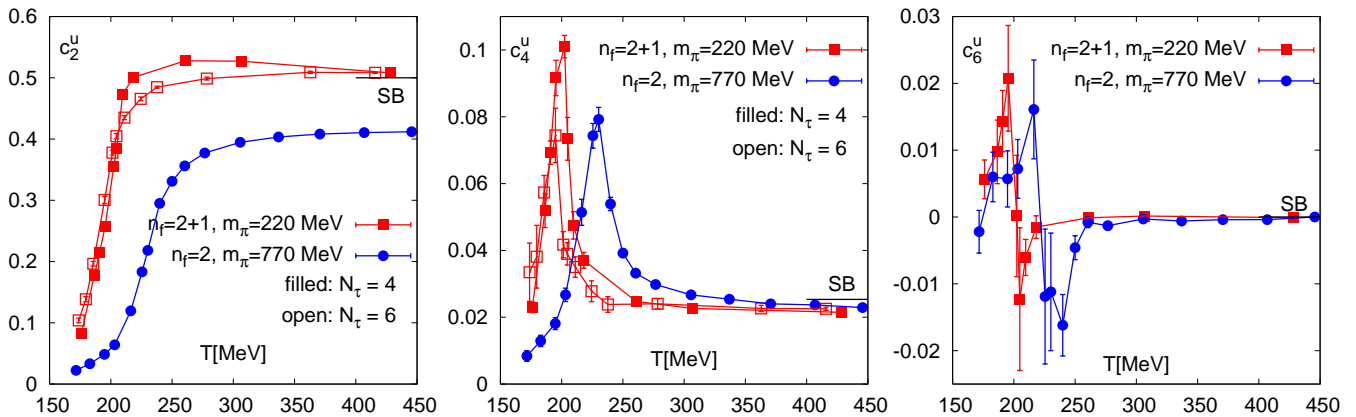


**Fig. 4.** Taylor coefficients of the pressure in term of the up-quark chemical potential. Results are obtained with the p4fat3 action on  $N_\tau = 4$  (full) and  $N_\tau = 6$  (open symbols) lattices. We compare preliminary results of (2+1)-flavor a pion mass of  $m_\pi \approx 220$  MeV to previous results of 2-flavor simulations with a corresponding pion mass of  $m_p \approx 770$  [16].

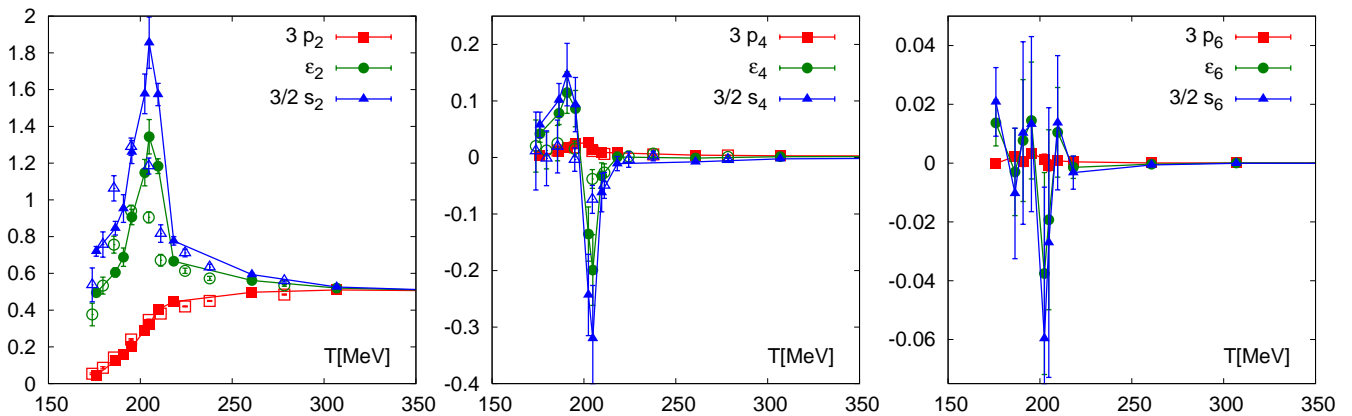


**Fig. 5.** Taylor coefficients of the pressure, the energy and entropy density with respect to the baryon chemical potential. Results are obtained with the p4fat3 action on  $N_\tau = 4$  (full) and  $N_\tau = 6$  (open symbols) lattices.

Combining Eqs. 9, 11, and 12 we then obtain the Taylor expansions for the energy and entropy densities [19]

$$\begin{aligned}
 \frac{\epsilon}{T^4} &= \sum_{n=0}^{\infty} (3c_n^B(T) + \bar{c}_n^B(T)) \left(\frac{\mu_B}{T}\right)^n \\
 &\equiv \sum_{n=0}^{\infty} \epsilon_n \left(\frac{\mu_B}{T}\right)^n, \\
 \frac{s}{T^3} &\equiv \frac{\epsilon + p - \mu_B n_B}{T^4} \\
 &= \sum_{n=0}^{\infty} ((4-n)c_n^B(T) + \bar{c}_n^B(T)) \left(\frac{\mu_B}{T}\right)^n \\
 &\equiv \sum_{n=0}^{\infty} s_n \left(\frac{\mu_B}{T}\right)^n.
 \end{aligned} \tag{13}$$

At present, we calculate the expansion coefficients  $\bar{c}_n^B$  from the coefficients  $c_n^B$ , in accordance with Eq. 12, by performing the  $T$  derivative numerically, which introduces a small systematic error.

In Fig. 5 we show the second, fourth and sixth order expansion coefficients of the pressure, energy density and entropy density as given in Eqs. 9 and 14, obtained with the p4fat3 action. Full symbols are from  $N_\tau = 4$  lattices, while the open symbols denote results from  $N_\tau = 6$  lattices. We again find small cut-off effects, however, higher order derivatives of pressure, energy density and entropy density with respect to  $\mu_B$  are still very preliminary, as the error bars are large. This is especially true for the results from  $N_\tau = 6$  lattices. Nevertheless, the overall pattern of the coefficients is in agreement with expectations based on an analysis of the singular behavior of the free energy, making use of an appropriate scaling Ansatz.

We find that the magnitude of the coefficients is decreasing drastically with increasing order, for all analyzed temperatures. Thus an approximation of the equation of state for small baryon chemical potential by means of a fourth or sixth order expansion seems to be justified. In general, an analysis of the radius of convergence of such a Taylor series is of great interest for an analysis of the QCD phase diagram, since the radius of convergence is

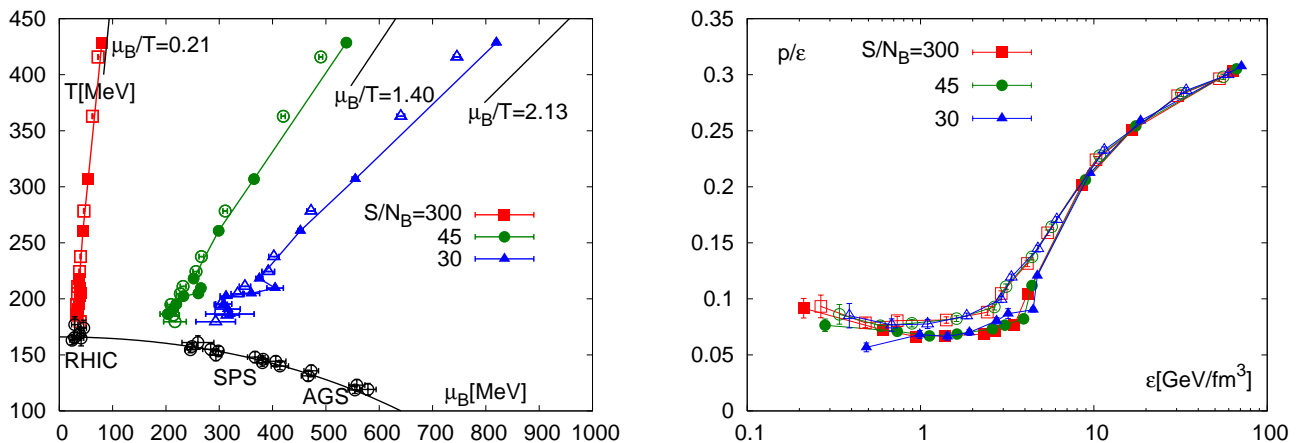


**Fig. 6.** On the left panel we show isentropic trajectories in the  $(T - \mu_B)$ -diagram, corresponding to  $s/n_B = 300, 45, 30$  respectively. Open symbols are from  $N_\tau = 6$ , obtained by a 4th order Taylor expansion of the pressure. Filled symbols are from  $N_\tau = 4$  calculations. We also show freeze-out data, as well as a parameterization of the freeze-out curve from [21]. Corresponding free gas limits are  $\mu_B/T = 0.21, 1.40, 2.13$  respectively and are indicated by solid lines. On the right panel we plot the ratio of pressure and energy density along those trajectories.

bounded by the location of the QCD critical point as well as by any first order phase transition line.

## 6 The isentropic equation of state

By using the Taylor expansion coefficients of the baryon number (Eq. 10) and entropy density (Eq. 14), we can compute the ratio of entropy per baryon number as function of  $T$  and  $\mu_B$ . Solving numerically for a constant ratio of entropy per baryon number,  $s/n_B$ , we determine isentropic trajectories in the  $(T, \mu_B)$ -plane. These trajectories are relevant for the description of matter created in relativistic heavy ion collisions. After equilibration the dense medium created in such a collision will expand along lines of constant entropy per baryon. It then is of interest to calculate thermodynamic quantities along such isentropic lines.

We find that isentropic expansion at high temperature is well represented by lines of constant  $\mu_B/T$  down to temperatures close to the transition,  $T \simeq 1.2T_0$ . In the low temperature regime we observe a bending of the isentropic lines in accordance with the expected asymptotic low temperature behavior. The isentropic expansion lines for matter created at SPS correspond to  $s/n_B \simeq 45$  while the isentropes at RHIC correspond to  $s/n_B \simeq 300$ . The energy range of the AGS which also corresponds to an energy range relevant for future experiments at FAIR/Darmstadt is well described by  $s/n_B \simeq 30$ . These lines are shown in Fig. 6 (left) together with data points characterizing the chemical freeze-out of hadrons measured at AGS, SPS and RHIC energies. These data points have been obtained by comparing experimental results for yields of various hadron species with hadron abundances in a resonance gas [20, 21]. The solid curve shows a phenomenological parameterization of these freeze-out data [21]. In general our

findings for lines of constant  $s/n_B$  are in good agreement with phenomenological model calculations that are based on combinations of ideal gas and resonance gas equations of state at high and low temperature, respectively [22, 23].

Results shown in Fig. 6 are based on a fourth order expansion of the pressure. We find, however, that the truncation error is small, i.e. the results change only little when we consider also the sixth order term in  $\mu_B$ . In accordance with the good convergence of our results, we find, that all trajectories shown in Fig. 6 (left) are well within the radius of convergence of the Taylor series. At present we estimate the radius of convergence of the pressure series to  $(\mu_B/T)^{\text{crit}} \gtrsim 2.7$ . The cut-off effects can be estimated by comparing open and full symbols.

We now proceed and calculate energy density and pressure on lines of constant entropy per baryon number using our Taylor expansion results up to  $\mathcal{O}(\mu_B^4)$ . We find that both quantities obtain corrections of about 10% at AGS (FAIR) energies ( $s/n_B = 30$ ) and high temperatures. The dependence of  $\epsilon$  and  $p$  on  $s/n_B$  cancels to a large extent in the ratio  $p/\epsilon$ , which is most relevant for the analysis of the hydrodynamic expansion of dense matter. This may be seen by considering the leading  $\mathcal{O}(\mu_B^2)$  correction,

$$\frac{p}{\epsilon} = \frac{1}{3} - \frac{1}{3} \frac{\epsilon_0 - 3p_0}{\epsilon_0} \left( 1 + \left[ \frac{\bar{c}_2}{\epsilon_0 - 3p_0} - \frac{\epsilon_2}{\epsilon_0} \right] \left( \frac{\mu_B}{T} \right)^2 \right). \quad (15)$$

In Fig. 6 (right) we show  $p/\epsilon$  as function energy density along our three isentropic trajectories. The softest point of the equation of state is found to be  $(p/\epsilon)_{\text{min}} \simeq 0.07 - 0.09$ , for  $N_\tau = 4$  and 6 respectively. Within our current numerical accuracy it is independent of  $s/n_B$ . Similar results for the asqtad action have been obtained in [18]. However, as our data is preliminary, the analysis clearly suffers from poor statistics, which is in particular true for our  $N_\tau = 6$  results.

## 7 Conclusions

We have presented results on the equation of state on lattices of  $N_\tau = 4, 6$  [1,14] and 8 [2] with two different kinds of improved staggered fermions. Our masses have been kept constant in physical units and are chosen such that we have a physical strange quark mass ( $m_s$ ) and 2 light quarks with a mass of  $m_l = 0.1m_s$ . We also presented some preliminary results with physical quark masses  $m_l = 0.05m_s$ . We find that our two actions lead to a consistent picture of the thermodynamics of QCD and find in particular for the  $N_\tau = 8$  results only small cut-off effects. We have calculated the equation of state as well as the velocity of sound and find the softest point of the equation of state to be  $(p/\epsilon)_{min} \simeq 0.09$  at energy densities of  $1 - 2 \text{ GeV}/\text{fm}^3$ .

Furthermore, we calculated corrections to the equation of state arising from a non-zero baryon chemical potential, by means of a Taylor expansion of the pressure. Within this framework we calculated the isentropic equation of state along lines of constant entropy per baryon number ( $s/n_B$ ) for RHIC, SPS and AGS (FAIR) energies. Within our current, preliminary, analysis we find the softest point of the equation of state to be independent of  $s/n_B$ .

## Acknowledgments

This work has been supported in part by contracts DE - AC02 - 98CH10886 and DE - FG02 - 92ER40699 with the U.S. Department of Energy. Numerical simulations have been performed on the BlueGene/L computers at Lawrence Livermore National Laboratory (LLNL) and the New York Center for Computational Sciences (NYCCS) as well as on the QCDOC computer of the RIKEN-BNL research center, the DOE funded QCDOC at Brookhaven National Laboratory (BNL) and the apeNEXT at Bielefeld University.

## References

1. M. Cheng *et al.*, Phys. Rev. D **77** (2008) 014511.
2. HotQCD Collaboration, in preparation.
3. C. Detar and R. Gupta [HotQCD Collaboration], PoS **LAT2007** (2007) 179; F. Karsch [RBC Collaboration and HotQCD Collaboration], arXiv:0804.4148 [hep-lat].
4. K. Symanzik, Nucl. Phys. B **226**, (1983) 187 and Nucl. Phys. B **226** (1983) 205.
5. S. Naik, Nucl. Phys. B **316** (1989) 238.
6. F. Karsch, E. Laermann and A. Peikert, Nucl. Phys. B **605** (2001) 579.
7. B. Sheikholeslami and R. Wohlert, Nucl. Phys. **259** (1985) 572.
8. P. Hasenfratz and F. Niedermayer, Nucl. Phys. B **414** (1994) 785; P. Hasenfratz and S. Hauswirth, K. Holland, T. Jorg, F. Niedermayer and U. Wenger, Int. J. Mod. Phys. C. **12** (2001) 691.
9. W. Bietenholz and U.-J. Wiese, Nucl. Phys. B **464** (1996) 319.
10. P. Hegde, F. Karsch, E. Laermann and S. Shcheredin, Eur. Phys. J. C **55** (2008) 423.
11. I. Hováth, A. D. Kennedy and S. Sint, Nucl. Phys. B **73** (1999) 834; M. A. Clark, A. D. Kennedy and Z. Sroczynski, Nucl. Phys. Proc. Suppl. **140** (2005) 835.
12. C. Aubin *et al.*, Phys. Rev. D **70** (2004) 094505.
13. A. Gray *et al.*, Phys. Rev. D **72** (2005) 094507.
14. C. Bernard *et al.*, Phys. Rev. D **75** (2007) 094505.
15. M.P. Lombardo, arXiv:0808.3101; C. Schmidt, PoS **LAT2006** (2006) 021.
16. C. R. Allton, M. Doring, S. Ejiri, S.J. Hands, O. Kaczmarek, F. Karsch, E. Laermann, K. Redlich, Phys. Rev. D **71** (2005) 054508.
17. C. R. Allton *et al.*, Phys. Rev. D **66** (2002) 074507; C. Miao and C. Schmidt, PoS **LAT2007** (2007) 175.
18. C. Bernard *et al.*, Phys. Rev. D **77** (2008) 014503.
19. S. Ejiri, F. Karsch, E. Laermann and C. Schmidt, Phys. Rev. D **73** (2006) 054506.
20. J. Cleymans and K. Redlich, Phys. Rev. Lett. **81** (1998) 5284; J. Cleymans and K. Redlich, Phys. Rev. C **60** (1999) 054908.
21. J. Cleymans, H. Oeschler and K. Redlich, S. Wheaton, Phys. Rev. C **73** (2006) 034905.
22. C. M. Hung and E. Shuryak, Phys. Rev. D **57** (1998) 1891.
23. V. D. Toneev, J. Cleymans, E. G. Nikonov, K. Redlich and A. A. Shanenko, J. Phys. G **27** (2001) 827.